PROPAGATION OF ONE AND TWO-DIMENSIONAL DISCRETE WAVES UNDER FINITE DIFFERENCE APPROXIMATION

Umberto Biccari
DeustoTech, Universidad de Deusto, Bilbao, Spain
Joint works with **Aurora Marica** (Politehnica University of Bucharest) and **Enrique Zuazua** (Universidad de Deusto, Universidad Autónoma de Madrid and Sorbonne Universités, Paris)

Craiova, July 6th, 2018

INTRODUCTION

Introduction

We analyze propagation properties of numerical waves obtained through a finite difference discretization on uniform or non-uniform meshes.

Our approach is based on the study of the propagation of high-frequency Gaussian beam solutions.

Basic idea

The energy of Gaussian beam solutions propagates along bi-characteristic rays, which are obtained from the Hamiltonian system associated to the symbol of the operator under consideration.

- CONTINUOUS SETTING: these techniques date back to Hörmander, and they have been extended by several authors (Gérard, Tartar, Wigner).
- DISCRETE SETTING: extension of micro-local techniques to the study of the propagation properties for discrete waves (Maciá, Marica, Zuazua).

Gaussian beams

$$\begin{cases} \rho(x)\partial_t^2 u(x,t) - div\big(\sigma(x)\nabla u(x,t)\big) = 0, & (x,t) \in \mathbb{R}^N \times (0,T) \\ u(x,0) = u^0(x), \quad \partial_t u(x,0) = u^1(x), & x \in \mathbb{R}^N \end{cases} \tag{1}$$

PRINCIPAL SYMBOL: $\mathcal{H}(x,t,\xi,\tau) = -\rho(x)\tau^2 + \sigma(x)|\xi|^2$

BI-CHARACTERISTIC RAYS: solutions to the first order ODE system

$$\begin{cases} \dot{x}(s) = \nabla_\xi \mathcal{H}(x(s),t(s),\xi(s),\tau(s)), & x(0) = x_0 \\ \dot{t}(s) = \partial_\tau \mathcal{H}(x(s),t(s),\xi(s),\tau(s)), & t(0) = 0 \\ \dot{\xi}(s) = -\nabla_x \mathcal{H}(x(s),t(s),\xi(s),\tau(s)), & \xi(0) = \xi_0 \\ \dot{\tau}(s) = -\partial_t \mathcal{H}(x(s),t(s),\xi(s),\tau(s)), & \tau(0) = \tau_0 \;\; s.t. \;\; \mathcal{H}(x_0,0,\xi_0,\tau_0) = 0. \end{cases}$$

Rays of geometric optics

$(t, x(t))$: projection of a bi-characteristic to the physical time-space domain.

$$u^{\varepsilon}(x,t) = \varepsilon^{1-\frac{N}{4}} a(x,t) e^{\frac{i}{\varepsilon}\phi(x,t)}$$

$$\phi(x,t) = \xi(t)(x - x(t)) + \frac{1}{2}(x - x(t))^T M(t)(x - x(t)), \quad \Im(M(t)) > 0$$

- u^{ε} is an approximate solution of the wave equation (1):

$$\sup_{t\in(0,T)} \|\Box u^{\varepsilon}(\cdot,t)\|_{L^2(R_x^N)} \leq C\varepsilon^{\frac{1}{2}}$$

- the energy of u^{ε} is bounded with respect to ε.
- the energy of u^{ε} is exponentially small off the ray $(x(t),t)$:

$$\sup_{t\in(0,T)} \int_{\mathbb{R}^N \setminus B(t)} |\rho u_t^{\varepsilon}|^2 + |\sigma \nabla u^{\varepsilon}|^2 \, dx \leq Ce^{-\beta/\sqrt{\varepsilon}}$$

$$\beta > 0, \; B(t) := B(x(t), \varepsilon^{\frac{1}{4}})$$

J. Ralston, Studies in Partial Differential Equations, 1982

F. Maciá and E. Zuazua, Asymptot. Anal., 2002

J. Rauch, X. Zhang and E. Zuazua, J. Math. Pures Appl., 2005

We study the problem on three levels:

- The **one-dimensional** wave equation with **constant** coefficients:

$$\partial_t^2 u - \partial_x^2 u = 0, \quad (x,t) \in (-1,1) \times (0,T);$$

- The **one-dimensional** wave equation with **variable** coefficients:

$$\rho(x)\partial_t^2 u - \partial_x(\sigma(x)\partial_x u) = 0, \quad (x,t) \in (-1,1) \times (0,T);$$

- The **two-dimensional** wave equation:

$$\rho(x,y)\partial_t^2 u - div(\sigma(x,y)\nabla u) = 0, \quad (x,y,t) \in (-1,1)^2 \times (0,T).$$

In all cases we will consider zero Dirichlet boundary condition.

Our principal aim is to illustrate that numerical high-frequency solutions can behave in unexpected manners, as a result of the accumulation of the local effects introduced by the heterogeneity of the numerical grid.

One-dimensional wave equation

Semi-discrete approximation

Uniform mesh

$$\mathcal{G}^h := \left\{ x_j := -1 + jh,\ j = 0, \ldots, N+1\ h = 2/(N+1),\ N \in \mathbb{N}^* \right\}$$

Non-uniform mesh

- $g \in C^2(\mathbb{R})$
- $0 < g_d^- \leq |g'(x)| \leq g_d^+ < +\infty$
- $|g''(x)| \leq g_{dd} < +\infty$

$$\Longrightarrow \quad \mathcal{G}_g^h := \left\{ g_j := g(x_j),\ x_j \in \mathcal{G}^h \right\}$$

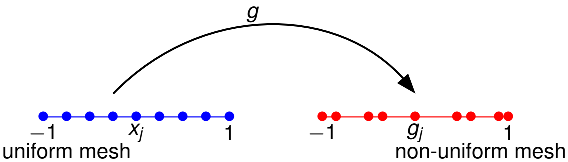

- $h_{j+1/2} := g_{j+1} - g_j, \quad j = 0, \dots, N$
- $h_{j-1/2} := g_j - g_{j-1}, \quad j = 1, \dots, N+1$
- $h_j := \frac{h_{j+1/2} + h_{j-1/2}}{2}, \quad j = 1, \dots, N$

Semi-discrete wave equation

$$\begin{cases} h_j u_j''(t) - \left(\dfrac{u_{j+1}(t) - u_j(t)}{h_{j+1/2}} - \dfrac{u_j(t) - u_{j-1}(t)}{h_{j-1/2}} \right) = 0 \\ u_0(t) = u_{N+1}(t) = 0 \\ u_j(0) = u_j^0, \quad u_j'(0) = u_j^1 \\ j = 1, \dots, N, \quad t \in (0, T). \end{cases}$$

Hamiltonian system

Hamiltonian

$$\mathcal{H}_c(x, t, \xi, \tau) = -\tau^2 + \xi^2$$

Bi-characteristic rays

$$\begin{cases} \dot{x}(s) = 2\xi(s), & x(0) = x_0 \\ \dot{t}(s) = -2\tau(s), & t(0) = 0 \\ \dot{\xi}(s) = 0, & \xi(0) = \xi_0 \\ \dot{\tau}(s) = 0, & \tau(0) = \tau_0 \;\; s.t. \;\; \mathcal{H}_c(x_0, 0, \xi_0, \tau_0) = 0. \end{cases}$$

- For any ξ_0 there are two characteristics starting from x_0: $x^{\pm}(t) = x_0 \mp t$.
- Each one of these characteristics reaches the boundary of $(-1, 1)$ in a uniform time and reflects according to the geometric optics laws.

Discrete Hamiltonian

$$\mathcal{H}(y,t,\xi,\tau) := -\tau^2 + c_g(y)^2\omega(\xi)^2$$
$$y = g^{-1}(x),\ \ c_g(y) := \frac{1}{g'(y)},\ \ \omega(\xi) := 2\sin\left(\frac{\xi}{2}\right)$$

Discrete bi-characteristic rays

$$\begin{cases} \dot{y}(s) = 2c_g(y(s))^2\omega(\xi(s))\partial_\xi\omega(\xi(s)), & y(0) = y_0 \\ \dot{t}(s) = -2\tau(s), & t(0) = 0 \\ \dot{\xi}(s) = -2c_g(y(s))\partial_y c_g(y(s))\omega(\xi(s))^2, & \xi(0) = \xi_0 \\ \dot{\tau}(s) = 0, & \tau(0) = \tau_0 \end{cases}$$

- $\partial_\xi\omega(\xi)$: **group velocity**, i.e. the speed at which the energy associated with wave number ξ moves.

- $\forall\, s,\ \tau(s) = \tau_0$
- $H(y(s), t(s), \xi(s), \tau(s)) = 0$

$\Rightarrow$ $\boxed{\tau_0^{\pm} = \pm c_g(y(s))|\omega(\xi(s))|}$

Since $\dot{t}(s) \neq 0$, the Inverse Function Theorem allows to parametrize the curve $s \mapsto (y(s), t(s), \xi(s), \tau_0^{\pm})$ by $t \mapsto (y(t), t, \xi(t), \tau_0^{\pm})$.

$$\begin{cases} \dot{y}^{\pm}(t) = \mp c_g(y^{\pm}(t))\partial_\xi \omega(\xi^{\pm}(t)) \\ \dot{\xi}^{\pm}(t) = \pm \partial_y c_g(y^{\pm}(t))\omega(\xi^{\pm}(t)) \\ y^{\pm}(0) = y_0, \quad \xi^{\pm}(0) = \xi_0 \end{cases}$$

- $c_g(\cdot) > 0$

$\Rightarrow$ $\boxed{|\dot{y}^{\pm}(t)| = c_g(y^{\pm}(t)) \left|\partial_\xi \omega(\xi^{\pm}(t))\right|}$

- The velocity of the rays vanishes if, and only if, $\partial_\xi(\omega) = \cos(\xi/2) = 0$, i.e. $\xi = (2k+1)\pi$, $k \in \mathbb{Z}$.
- When $\omega(\xi) = \xi$, corresponding to the continuous case, this cannot happen.

Numerical results

- $\mathbf{x}^h$: uniform mesh of size $h = 2/(N+1)$.
- $\mathbf{g}^{h,1} := \tan\left(\frac{\pi}{4}\mathbf{x}^h\right)$ and $\mathbf{g}^{h,2} := 2\sin\left(\frac{\pi}{6}\mathbf{x}^h\right)$: non-uniform grids

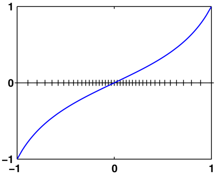

$\mathbf{g}^{\mathbf{h},1}$

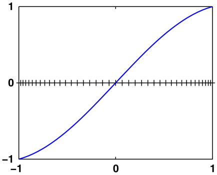

$\mathbf{g}^{\mathbf{h},2}$

Time discretization: **leap-frog scheme** with CFL condition $\delta t = 0.1 \cdot h$

Initial data built from a Gaussian profile:

$$\boxed{G_\gamma(x) = e^{-\frac{\gamma}{2}\left(g^{-1}(x) - g^{-1}(x_0)\right)^2} e^{i\frac{\xi_0}{h}g^{-1}(x)}, \quad u^0(x) = G_\gamma(x), \quad u^1(x) = (u^0)'(x).}$$

Hamiltonian system in the x variable

$$\begin{cases} \dot{x}^{\pm}(t) = \mp a_g(x^{\pm}(t)) \cos\left(\dfrac{\xi^{\pm}(t)}{2}\right), & x^{\pm}(0) = x_0 \\ \dot{\xi}^{\pm}(t) = \pm 2 b_g(x^{\pm}(t)) \sin\left(\dfrac{\xi^{\pm}(t)}{2}\right), & \xi^{\pm}(0) = \xi_0. \end{cases}$$

$$a_g(\cdot) := (g' c_g)(g^{-1}(\cdot)),\ b_g(\cdot) := c_g'(g^{-1}(\cdot)),\ x_0 = g(y_0).$$

- Independently of the choice of the function g, we always have $\mathbf{a_g \equiv 1}$.
- For each mesh refinement, b_g can be computed explicitly:

▷ $g(y) = \tan\left(\frac{\pi}{4} y\right) \quad \Rightarrow \quad \boxed{b_g(x) = -\dfrac{2x}{x^2+1}}$

▷ $g(y) = 2\sin\left(\frac{\pi}{6} y\right) \quad \Rightarrow \quad \boxed{b_g(x) = \dfrac{x}{4-x^2}}$

Phase portrait

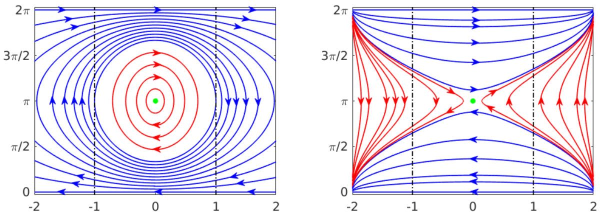

EQUILIBRIUM: $P_{\mathrm{e}} := (x_{\mathrm{e}}, \xi_{\mathrm{e}}) = (0, \pi)$

- tangential mesh (left): **CENTER** (stable equilibrium)
- sinusoidal mesh (right): **SADDLE** (unstable equilibrium)

Remark

The solutions of the semi-discrete wave equation may be written as linear combinations of monochromatic waves given by the complex exponentials

$$e^{\pm ij\left(\frac{\sqrt{\lambda_j}}{j\pi}t - x\right)}, \quad \lambda_j(h) = \frac{4}{h^2}\sin^2\left(\frac{j\pi h}{2}\right), \quad j \in 1 \ldots N.$$

In view of that, the relevant range of frequencies for the semi-discrete waves is $\xi \in [0, \pi]$, and the most suitable choice for the domain of the phase variable in the finite difference setting would be $\xi \in [-\pi, \pi]$, for taking into account the two branches of the associated bi-characteristic rays.

Consequently, the phase diagrams have to be interpreted as showing in the upper part $\xi \in [\pi, 2\pi]$ what would actually correspond to $\xi \in [-\pi, 0]$.

Plots

At low frequencies, the numerical solutions behave like the continuous ones: they propagate along straight characteristic lines and reflect following the Descartes-Snell's law when they touch one of the two endpoints.

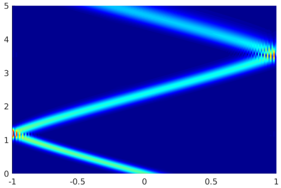

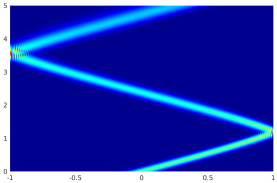

Propagation of a Gaussian wave packet with initial frequency $\xi_0 = \pi/4$ (left) and $\xi_0 = 7\pi/4$ (right), employing the mesh $\mathbf{g}^{h,1}$.

High-frequency pathologies

NON-PROPAGATING WAVES $(x_0 = 0, \xi_0 = \pi)$

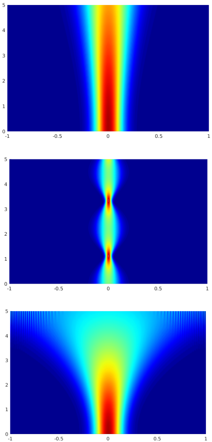

JUSTIFICATION

- The non propagating waves correspond to the equilibrium point P_e on the phase diagram.
- For $\xi = \pi$ we have $\partial_\xi \omega(\xi) = 0$ and, therefore, the velocity of the rays vanishes.

INTERNAL REFLECTION

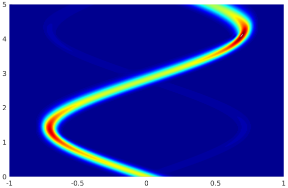

$x_0 = 0,\ \xi_0 = \frac{7\pi}{15}$, mesh $\mathbf{g}^{\mathbf{h},\mathbf{1}}$

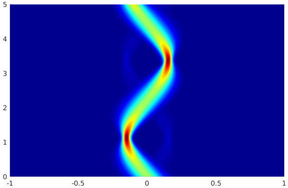

$x_0 = 0,\ \xi_0 = \frac{13\pi}{15}$, mesh $\mathbf{g}^{\mathbf{h},\mathbf{1}}$

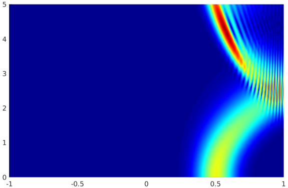

$x_0 = \frac{1}{2},\ \xi_0 = \pi$, mesh $\mathbf{g}^{\mathbf{h},\mathbf{2}}$

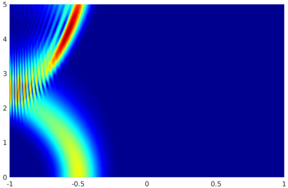

$x_0 = -\frac{1}{2},\ \xi_0 = \pi$, mesh $\mathbf{g}^{\mathbf{h},\mathbf{2}}$

JUSTIFICATION

- On the mesh $\mathbf{g}^{h,1}$, approaching the endpoints of the domain the step size increases and the group velocity $1/h$ of the high-frequency waves decreases. If this group velocity vanishes before the wave has reached the boundary, then this results in a process of internal reflection.
- For the mesh $\mathbf{g}^{h,2}$, P_{e} is a saddle point, and the red curves always remain trapped either in the region $x \in [0,1]$ or $x \in [-1,0]$.
- The amplitude of the wave is the one of the Gaussian profile of the initial datum, which is of the order of $h^{-0.9}$. On the mesh $\mathbf{g}^{h,1}$, while approaching the boundary h increases. Therefore, the support of the ray shrinks and, due to energy conservation, the high of the corresponding wave has to increase.

Variable coefficients wave equation

$$\begin{cases} \rho(x)\partial_t^2 u - \partial_x\big(\sigma(x)\partial_x u\big) = 0, & (x,t) \in (-1,1)\times(0,T) \\ u(-1,t) = u(1,t) = 0, & t \in (0,T) \\ u(x,0) = u^0(x), \quad \partial_t u(x,0) = u^1(x), & x \in (-1,1), \end{cases}$$

$\rho, \sigma \in L^\infty(\mathbb{R})$ with $\rho(x) \geq \rho^* > 0$ and $\sigma(x) \geq \sigma^* > 0$.

PRINCIPAL SYMBOL: $\mathcal{H}_c(x,t,\xi,\tau) = -\rho(x)\tau^2 + \sigma(x)\xi^2$

BI-CHARACTERISTIC RAYS: solutions to the first order ODE system

$$\begin{cases} \dot{x}(s) = 2\sigma(x(s))\xi(s), & x(0) = x_0 \\ \dot{t}(s) = -2\rho(x(s))\tau(s), & t(0) = 0 \\ \dot{\xi}(s) = \rho'(x(s))\tau^2(s) - \sigma'(x(s))\xi^2(s), & \xi(0) = \xi_0 \\ \dot{\tau}(s) = 0, & \tau(0) = \tau_0 \;\; s.t. \;\; \mathcal{H}_c(x_0, 0, \xi_0, \tau_0) = 0. \end{cases}$$

Notice that the bi-characteristics are not straight lines, since $\dot{\xi}(s) \neq 0$.

Discrete Hamiltonian

$$\mathcal{H}(y,t,\xi,\tau) := -\tau^2 + c_g(y)^2\omega(\xi)^2$$

$$y = g^{-1}(x), \quad c_g(y) := \frac{1}{g'(y)}\sqrt{\frac{\sigma(g(y))}{\rho(g(y))}}, \quad \omega(\xi) := 2\sin\left(\frac{\xi}{2}\right)$$

Discrete bi-characteristic rays

$$\begin{cases} \dot{y}^{\pm}(t) = \mp c_g(y^{\pm}(t))\partial_\xi\omega(\xi^{\pm}(t)), & y^{\pm}(0) = y_0 \\ \dot{\xi}^{\pm}(t) = \pm\partial_y c_g(y^{\pm}(t))\omega(\xi^{\pm}(t)), & \xi^{\pm}(0) = \xi_0. \end{cases}$$

Numerical results

COEFFICIENTS: $\rho(x) \equiv 1$ and $\sigma(x) = 1 + A\cos^2(\kappa\pi x)$, $A > 0$, $\kappa \in \mathbb{N}^*$.

Hamiltonian system

$$\begin{cases} \dot{x}(t) = -\sqrt{1 + A\cos^2(\kappa\pi x(t))}\cos\left(\dfrac{\xi(t)}{2}\right), & x(0) = x_0 \\ \dot{\xi}(t) = F_j^{A,\kappa}(x(t))\sin\left(\dfrac{\xi(t)}{2}\right), & \xi(0) = \xi_0, \quad j = 0, 1, 2. \end{cases}$$

- $j = 0$: uniform mesh
- $j = 1$: tangential mesh
- $j = 2$: sinusoidal mesh

Plots

LOW-FREQUENCY SOLUTIONS $(\xi_0 = \pi/7)$:

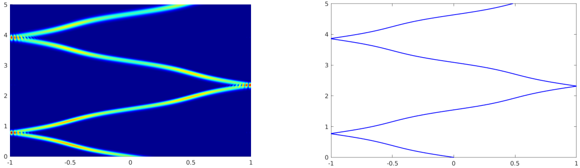

$A = 2$, $\kappa = 1$.

- The wave travels along characteristics and reaches the boundary, where it is reflected according to the Descartes-Snell's law.
- The parameters A and κ in the coefficient σ affect the shape of the rays.

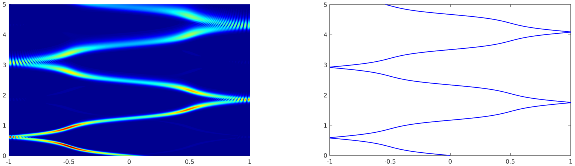

$A = 7$, $\kappa = 1$.

- $A_1 \geq A_2 \quad \Rightarrow \quad |\dot{x}_{A_1,\kappa}(t)| \geq |\dot{x}_{A_2,\kappa}(t)|, \quad |\ddot{x}_{A_1,\kappa}(t)| \geq |\ddot{x}_{A_2,\kappa}(t)|$

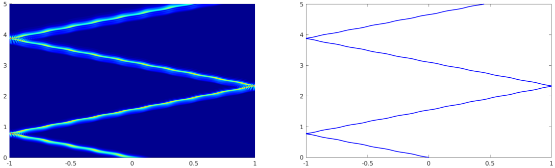

$A = 2$, $\kappa = 5$.

- σ is a periodic function of period $T = 2\kappa$.

High-frequency pathologies

In what follows, we will always assume $A = 1$ and $\kappa = 1$ in the coefficient σ.

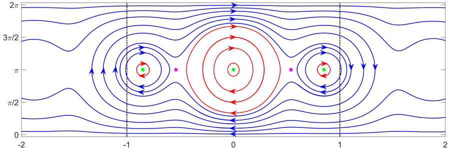

Mesh $\mathbf{g}^{\mathbf{h},1}$

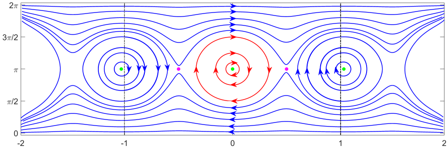

Mesh $\mathbf{g}^{\mathbf{h},2}$

NON PROPAGATING WAVES:

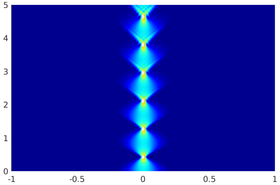

$x_0 = 0$, $\xi_0 = \pi$, mesh $\mathbf{g}^{\mathbf{h},1}$

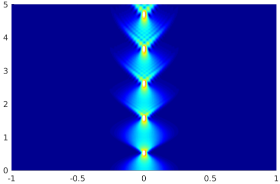

$x_0 = 0$, $\xi_0 = \pi$, mesh $\mathbf{g}^{\mathbf{h},2}$

INTERNAL REFLECTION:

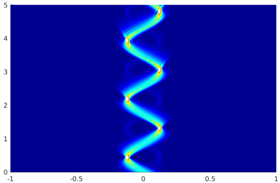

$x_0 = 0$, $\xi_0 = \frac{4\pi}{5}$, mesh $\mathbf{g}^{\mathbf{h},1}$

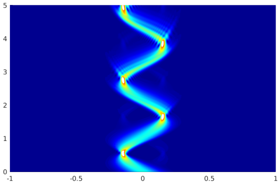

$x_0 = 0$, $\xi_0 = \frac{4\pi}{5}$, mesh $\mathbf{g}^{\mathbf{h},2}$

- We have several different initial positions which, at frequency $\xi_0 = \pi$, generate non propagating waves.

x_0 =unstable equilibrium
$\xi_0 = \pi$, mesh $\mathbf{g}^{\mathbf{h},\mathbf{1}}$

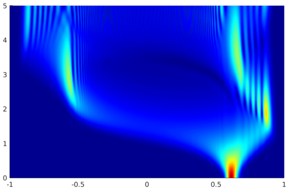

- Initial data corresponding to one of the unstable fixed point produce solutions that, apart from showing absence of propagation, present also a huge dispersion.
- These solutions, as soon as they move away from the unstable equilibrium point, are quite immediately affected by the orbits around the stable ones, thus generating the comeback effects that can be appreciated in the figure.

TWO-DIMENSIONAL WAVE EQUATION

Two-dimensional wave equation

$$\begin{cases} \rho(\mathbf{z})\partial_t^2 u - div_{\mathbf{z}}\big(\sigma(\mathbf{z})\nabla_{\mathbf{z}} u\big) = 0, & (\mathbf{z}, t) \in \Omega \times (0, T) \\ u|_{\partial\Omega} = 0, & t \in (0, T) \\ u(\mathbf{z}, 0) = u^0(\mathbf{z}), \quad \partial_t u(\mathbf{z}, 0) = u^1(\mathbf{z}), & \mathbf{z} \in \Omega, \end{cases}$$

- $\mathbf{z} := (x, y)$
- $\Omega := (-1, 1)^2$
- $\rho, \sigma \in L^\infty(\Omega)$ with $\rho(\mathbf{z}) \geq \rho^* > 0$ and $\sigma(\mathbf{z}) \geq \sigma^* > 0$.

Semi-discrete approximation

Uniform mesh

$$\mathbf{G}^h := \Big\{ \mathbf{z}_{j,k} := (x_j, y_k) = (-1 + jh_x, -1 + kh_y),$$
$$j = 0, \ldots, M+1, k = 0, \ldots, N+1 \Big\}$$

Non-uniform mesh

g_1, g_2: diffeomorphisms of Ω $\quad \Rightarrow \quad \mathbf{G}^h_{\mathbf{g}} := \Big\{ \boldsymbol{\omega}_{j,k} := (\upsilon_j, \zeta_k) = (g_1(x_j), g_2(y_k)) \Big\}$

Hamiltonian system

Discrete Hamiltonian

$$\mathcal{P}(x,y,t,\xi,\eta,\tau) := \tau^2 - \Lambda(x,y,\xi,\eta)$$
$$\Lambda(x,y,\xi,\eta) := \frac{\sigma(x,y)}{\rho(x,y)}\left(4\sin^2\left(\frac{\xi}{2}\right)\frac{1}{g_1'(x)^2} + 4\sin^2\left(\frac{\eta}{2}\right)\frac{1}{g_2'(y)^2}\right).$$

Discrete bi-characteristic rays

$$\begin{cases} \dot{\mathbf{z}}_e(s) = \nabla_{\boldsymbol{\theta}_e}\mathcal{P}(\mathbf{z}_e(s),\boldsymbol{\theta}_e(s)), & \mathbf{z}_e(0) = \mathbf{z}_e^0 := (x_0,y_0,t_0) \\ \dot{t}(s) = 2\tau(s), & t(0) = 0 \\ \dot{\boldsymbol{\theta}}_e(s) = -\nabla_{\mathbf{z}_e}\mathcal{P}(\mathbf{z}_e(s),\boldsymbol{\theta}_e(s)), & \boldsymbol{\theta}_e(0) = \boldsymbol{\theta}_e^0 := (\xi_0,\eta_0,\tau_0) \\ \dot{\tau}(s) = 0, & \tau(0) = \tau_0. \end{cases}$$

$$\mathbf{z}_e := (x,y,t), \quad \boldsymbol{\theta}_e := (\xi,\eta,\tau)$$

Assume $\rho = \sigma \equiv 1$.

HAMILTONIAN SYSTEM IN THE x COMPONENT:

$$\begin{cases} \dot{x}^{\pm}(t) = \mp \frac{r_1}{r_0} g_1'(g_1^{-1}(x^{\pm}(t)))\partial_{\xi}\lambda_1(g_1^{-1}(x^{\pm}(t)), \xi^{\pm}(t)) \\ \dot{\xi}^{\pm}(t) = \mp \frac{r_1}{r_0} \partial_x \lambda_1(g_1^{-1}(x^{\pm}(t)), \xi^{\pm}(t)) \end{cases}$$

HAMILTONIAN SYSTEM IN THE y COMPONENT:

$$\begin{cases} \dot{y}^{\pm}(t) = \mp \frac{r_2}{r_0} g_2'(g_2^{-1}(y^{\pm}(t)))\partial_{\eta}\lambda_2(g_2^{-1}(y^{\pm}(t)), \eta^{\pm}(t)) \\ \dot{\eta}^{\pm}(t) = \mp \frac{r_2}{r_0} \partial_y \lambda_2(g_2^{-1}(y^{\pm}(t)), \eta^{\pm}(t)). \end{cases}$$

- $r_0 := \sqrt{\Lambda(\mathbf{z}^{\pm}(t), \boldsymbol{\theta}^{\pm}(t))}, \quad r_1 := \lambda_1(x^{\pm}(t), \xi^{\pm}(t)), \quad r_2 := \lambda_2(y^{\pm}(t), \eta^{\pm}(t)),$
- $\lambda_1(x, \xi) := 2\sin\left(\frac{\xi}{2}\right)\frac{1}{g_1'(x)}, \quad \lambda_2(y, \eta) := 2\sin\left(\frac{\eta}{2}\right)\frac{1}{g_2'(y)}.$

MESH FUNCTIONS: $g_1(x) = g_2(x) = \tan\left(\frac{\pi}{4}x\right) =: g(x)$

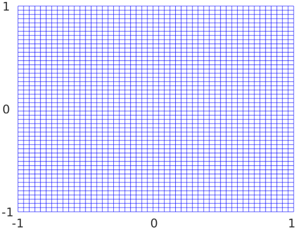

Uniform grid

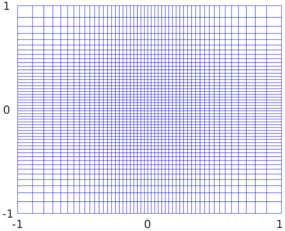

Non-uniform grid

Solution in Fourier series

$$\mathbf{u^h} = \sum_{j=1}^{M} \sum_{k=1}^{N} \beta_{j,k} \boldsymbol{\Phi}_{j,k}(\boldsymbol{\omega})\, e^{it\sqrt{\lambda_{j,k}}}.$$

- $\boldsymbol{\omega} := (\upsilon, \zeta)$
- $\{\boldsymbol{\Phi}_{j,k}, \lambda_{j,k}\}$ are the eigenvector and the eigenvalues of the discrete Laplacian $-\Delta_\omega$ on the refined mesh $\mathbf{G}^h_\mathbf{g}$

$$-\Delta_\omega \boldsymbol{\Phi}_{j,k} = \lambda_{j,k} \boldsymbol{\Phi}_{j,k}, \quad j = 1, \ldots, M, \quad k = 1, \ldots, N.$$

- $\beta_{j,k}$: corresponding Fourier coefficients of the initial datum $\mathbf{u}^{0,\mathbf{h}}$.

INITIAL DATUM:

$$u^0(x,y) = \exp\left[-\gamma\left((x-x_0)^2 + (y-y_0)^2\right)\right] \exp\left[i\left(\frac{x\xi_0}{h} + \frac{y\eta_0}{h}\right)\right]$$

$\gamma := h^{-0.9}$.

Plots

At low frequencies, the solution remains concentrated and propagates along straight characteristics which reach the boundary, where there is reflection according to the Descartes-Snell's law. This independently on whether we use a uniform or a non-uniform mesh.

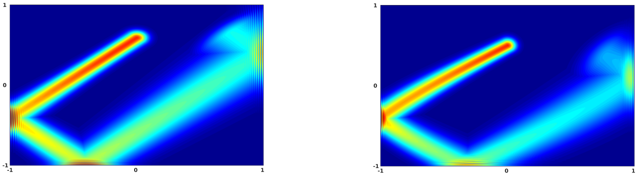

Numerical solutions with parameters $(x_0, y_0, \xi_0, \eta_0) = (0, 1/2, \pi/4, \pi/4)$. The discretization is done on a uniform mesh (left) and on a non-uniform one obtained through the mesh function **g** (right).

High frequency pathologies

NON PROPAGATING WAVES:

- $(x_0, y_0, \xi_0, \eta_0) = (1, 0, \pi/2, \pi)$, uniform (left) and non-uniform (right) mesh

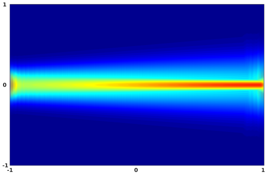

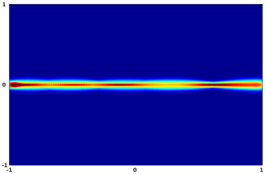

- $(x_0, y_0, \xi_0, \eta_0) = (0, 0, \pi, \pi)$, uniform (left) and non-uniform (right) mesh

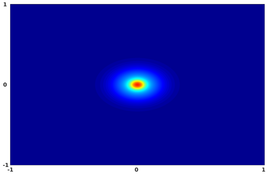

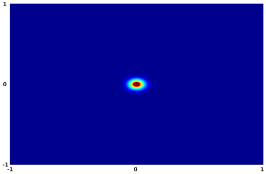

JUSTIFICATION:

Hamiltonian system in the x/y direction

$$\begin{cases} \dot{x}(t) = -\dfrac{4}{r_0\pi}\sin(\xi(t))\dfrac{1}{x(t)^2+1} \\ \dot{\xi}(t) = -\dfrac{32}{r_0\pi}\sin^2\left(\dfrac{\xi(t)}{2}\right)\dfrac{x(t)}{(x(t)^2+1)^2} \end{cases} \qquad \begin{cases} \dot{y}(t) = -\dfrac{4}{r_0\pi}\sin(\eta(t))\dfrac{1}{y(t)^2+1} \\ \dot{\eta}(t) = -\dfrac{32}{r_0\pi}\sin^2\left(\dfrac{\eta(t)}{2}\right)\dfrac{y(t)}{(y(t)^2+1)^2}. \end{cases}$$

$P_e := (0,\pi)$: unique equilibrium for both systems.

- $(x_0, y_0, \xi_0, \eta_0) = (0, y_0, \pi, \eta_0)$: the corresponding solution does not propagates in the vertical direction.
- $(x_0, y_0, \xi_0, \eta_0) = (x_0, 0, \xi_0, \pi)$: the corresponding solution does not propagates in the horizontal direction.
- $(x_0, y_0, \xi_0, \eta_0) = (0, 0, \pi, \pi)$: the corresponding solution does not propagates neither in the vertical nor in the horizontal direction.

INTERNAL REFLECTION:

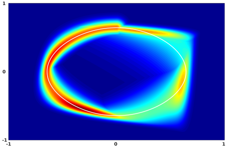

(a)

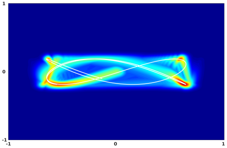

(b)

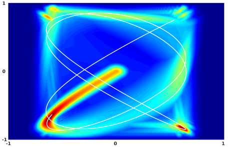

(c)

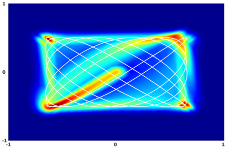

(d)

	x_0	y_0	ξ_0	η_0	T
Figure (a)	0	$\tan(\arccos(\sqrt[4]{1/2}))$	$\pi/2$	π	$8s$
Figure (b)	0	0	$\pi/2$	$5\pi/6$	$21s$
Figure (c)	0	0	$\pi/2$	$7\pi/18$	$37s$
Figure (d)	0	0	$\pi/2$	$7\pi/12$	$118s$

Final remarks

Motivations for the study presented

This study is motivated by **control theory**[1] and **inverse problems**.[2, 3]

- Boundary controllability and identifiability properties of solutions of wave equations hold because of the fact that the energy is driven by characteristics that reach a subregion of the domain or of its boundary where the controllers or observers are placed.

In the framework of wave-like processes, observability is guaranteed by the **geometric control condition** (GCC), requiring all rays of geometric optics to enter the control region during the control time.

[1] C. Bardos, G. Lebeau and J. Rauch, SIAM J. Control Optim., 1992

[2] L. Baudouin and S. Ervedoza, SIAM J. Control Optim., 2013

[3] L. Baudouin, S. Ervedoza and A. Osses, J. Math. Pures Appl., 2015

When the wave equation is approximated by **finite difference methods**, observability/controllability may be lost under numerical discretization as the mesh size tends to zero, due to the existence of **high-frequency spurious solutions** for which the group velocity vanishes.

These high-frequency solutions are such that the energy concentrated in the control region is asymptotically smaller than the total energy, and we have **exponential blow-up** of the observability constant as $h \to 0$.

Several authors worked on the topic: Castro, Ervedoza, Glowinski, Ignat, Infante, Lions, Maciá, Marica, Micu, Zuazua,...

POSSIBLE REMEDIES: **Tikhonov regularization** (Glowinski), **filtering mechanisms** (Infante and Zuazua), **FE** (Castro and Micu), **two-grid algorithms** (Ignat, Negreanu and Zuazua).

THANK YOU FOR YOUR ATTENTION!

This project has received funding from the European Research Council (ERC) under the European Union's Horizon 2020 research and innovation program (grant agreement No 694126-DYCON).